Nucleophilically enhanced oxidatively promoted carbonylation of the iron(II) complexes .eta.-Cp(CO)(PR3)FeMe. Applications of the quantitative analysis of ligand effects

David C. Woska, Joshua Bartholomew, Jack E. Greene, Klaas Eriks, Alfred Prock, and Warren P. Giering

Organometallics, **1993**, 12 (2), 304-309• DOI: 10.1021/om00026a015 • Publication Date (Web): 01 May 2002

Nucleophilically Enhanced Oxidatively Promoted Carbonylation of the Iron(II) Complexes η-Cp(CO)(PR$_3$)FeMe. Applications of the Quantitative Analysis of Ligand Effects

David C. Woska, Joshua Bartholomew, Jack E. Greene, Klaas Eriks, Alfred Prock,* and Warren P. Giering*

Department of Chemistry, Metcalf Center for Science and Engineering, Boston University, Boston, Massachusetts 02215

Received July 10, 1992

The oxidatively promoted carbonylation of 11 iron(II) complexes, η-Cp(CO)(L)FeMe (L = PMe$_2$Ph, PMePh$_2$, PEtPh$_2$, P(*p*-XPh)$_3$ (X = Me, MeO, H, F, Cl), PCyPh$_2$, PCy$_2$Ph, PCy$_3$) in methylene chloride (0.1 M tetrabutylammonium hexafluorophosphate, 0 °C, 1 atm CO) is enhanced when small amounts of acetonitrile (AN) are added to the reaction mixture. At higher [AN], the reaction is inhibited and the rate approaches the rate observed when AN is the solvent. A proposed mechanism includes as a key step the interconversion of η-Cp(AN)(L)-FeCOMe$^+$ to a reactive complex which subsequently reacts with CO. Rate constants or ratios of rate constants for the individual steps were determined by computer simulation of square wave and cyclic voltammetry data. Quantitative analysis of the ligand effect data shows that the reversible conversion of η-Cp(AN)(L)FeCOMe$^+$ to this reactive intermediate is insensitive to the electronic properties of L but is facilitated by increasing size of L. The partitioning of the intermediate between η-Cp(CO)(L)FeCOMe$^+$ and η-Cp(AN)(L)FeCOMe$^+$ is enhanced by ligands that are better electron donors. The steric profile shows sequential regions of no steric effects, steric acceleration, and steric inhibition.

Introduction

In previous papers,[1,2] we showed that the electrochemically initiated redox-catalyzed carbonylation of the robust complexes η-Cp(CO)(L)FeMe proceeds via an alkyl to acyl rearrangement of the iron(III) complexes η-Cp(CO)(L)-FeMe$^+$. We suggested that in CH_2Cl_2 the rate-limiting step in the carbonylation process is the entering ligand (CH_2Cl_2 or PF_6^-, from the supporting electrolyte) assisted rearrangement which is followed by the rapid displacement of the entering ligand by CO.[1] In acetonitrile (AN), the entering ligand (AN) assisted rearrangement is fast and it appears that the second, and rate-determining step, is the displacement of AN by CO.[2] We noted that we could not distinguish between a direct reaction of η-Cp(AN)-(L)FeCOMe$^+$ with CO and a rapid preequilibrium between η-Cp(AN)(L)FeCOMe$^+$ and some transient complex (i.e. η-Cp(CH_2Cl_2)(L)FeCOMe$^+$, η-Cp(PF_6)(L)FeCOMe, or the η^2-acyl complex, η-Cp(L)Fe-η^2-(COMe)$^+$) which then reacted with CO.

Herein, we describe our electrochemical studies of the rate of carbonylation of η-Cp(CO)(L)FeMe$^+$ when AN is added to the methylene chloride reaction mixture. The observed enhancements of the carbonylation reaction at low concentrations of AN support the involvement of a transient intermediate.

Experimental Section

General Methods. The preparation of the complexes η-Cp-(CO)(L)FeMe and the purification of solvents has been described previously.[1] All the electrochemical experiments described herein were performed at 0 °C starting with methylene chloride containing 0.1 M TBAH and under 1 atm of CO. The concentration of carbon monoxide (7.9 ± 0.3 mM) in AN was determined as previously described for CH_2Cl_2 (7.9 ± 0.3 mM).[1] We have assumed that [CO] remained invariant as we changed the composition of the solvent. [CO] was always more than 10 times greater than the initial concentration of η-Cp(CO)(L)FeMe. The characterization of η-Cp(AN)(PPh$_3$)FeCOMe$^+$ was reported previously.[3]

Electrochemistry and Computer Simulation Methods. The apparent rate constant, k_{obs}, for the transformation of 1$^+$ and 2$^+$ and the rate constants or ratios of rate constants (Scheme I) were determined by computer simulation of square wave voltammetry data (SW) data.[1,2]

The SW electrochemical experiment consists of a positive scan which passes through the reduction potentials of 1$^+$/1 and 2$^+$/2 in turn, producing two current peaks (i_1 and i_2, respectively; see Figure 1). (During the course of the experiment, complex 2 is generated in situ by the electrochemically promoted carbonylation of 1; see Scheme I.) We measure the peak potentials (and the valley between) and their relative heights, as a function of scan rate and concentration of acetonitrile.

We did two types of simulations. In the first, we merely calculated the apparent pseudo-first-order rate constant, k_{obs}, for the 1$^+$ and 2$^+$ conversion.

$$\eta\text{-Cp(CO)(L)FeMe}^+ + \text{CO} \xrightarrow{k_{obs}} \eta\text{-Cp(CO)(L)FeCOMe}^+ \quad (1)$$

This allowed us to probe, in a simple way, the manner in which the overall reaction responds to variations in the solvent composition and the stereoelectronic properties of the ancillary phosphorus(III) ligands.[4] The second type of simulation is based on the chemistry shown in Scheme I. By considering the response of the carbonylation process to variations in [AN], we were able

(1) Prock, A.; Giering, W. P.; Greene, J. E.; Meirowitz, R. E.; Hoffman, S. L.; Woska, D. C.; Wilson, M.; Chang, R.; Chen, J.; Magnuson, R. H.; Eriks, K. *Organometallics* **1991**, *10*, 3479-3485.

(2) Woska, D. C.; Wilson, M.; Bartholomew, J.; Eriks, K.; Prock, A.; Giering, W. P. *Organometallics* **1992**, *11*, 3343-3352.

(3) Magnuson, R. H.; Meirowitz, R. E.; Zulu, S. J.; Giering, W. P. *J. Am. Chem. Soc.* **1982**, *104*, 5790.

0276-7333/93/2312-0304$04.00/0

Scheme I [a]

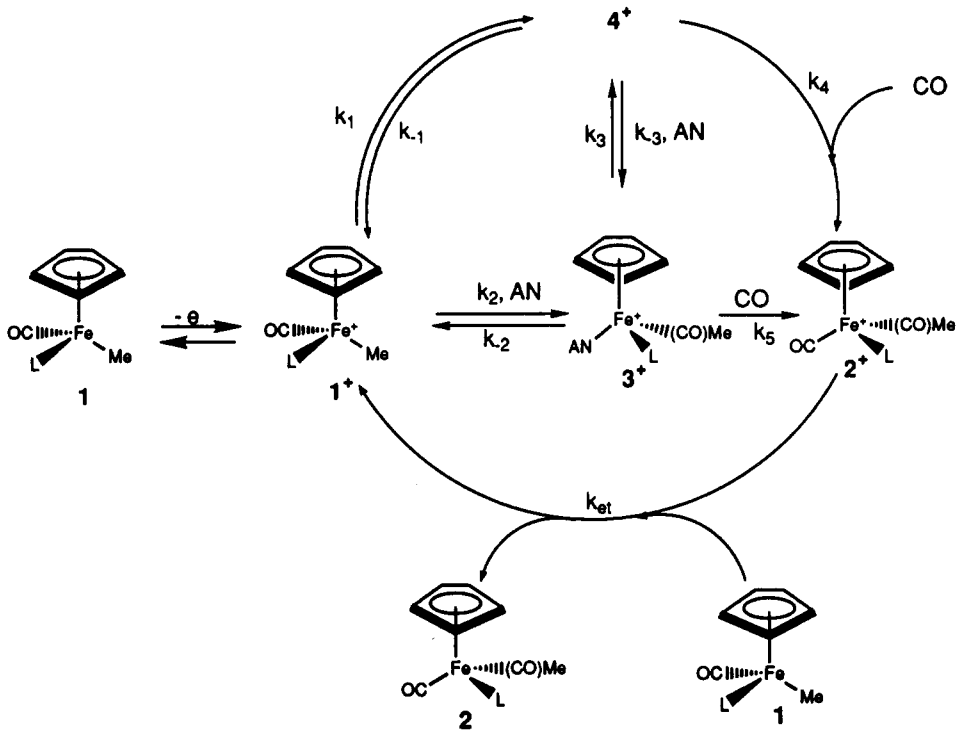

[a] No stereochemistry is intended.

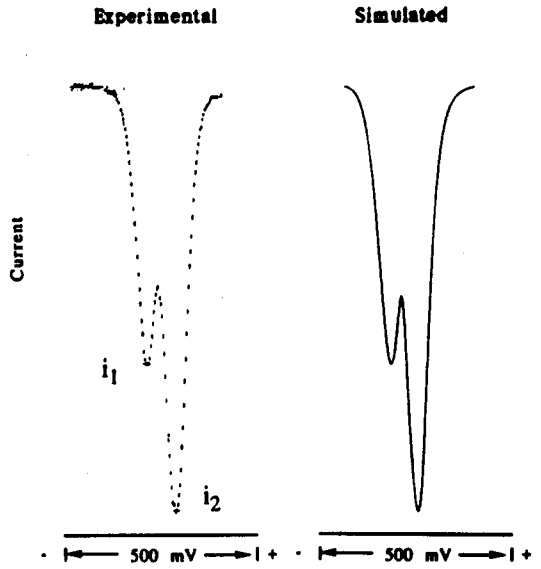

Figure 1. Experimental and simulated square wave voltammograms showing the current peaks, i_1 and i_2, for the electrochemical oxidation of η-Cp(CO)(PPh$_3$)FeMe in CH_2Cl_2 (0.1 M TBAH, 0 °C) containing 7.7 mM AN under 1 atm of CO. The scan rate was 0.02 V s^{-1}.

to extract the rate constant k_3 and the ratio k_4/k_{-3}. The other rate constants that appear in Scheme I were determined from separate experiments. For example, k_2 and k_{-2} for the interconversion of 1^+ and 3^+ were obtained via CV experiments in the absence of CO with mixtures of CH_2Cl_2 and AN. The values of k_1 and k_5 were obtained separately from SW studies of the carbonylation of η-Cp(CO)(L)FeMe$^+$ in CH_2Cl_2 solution[1] and in AN solution.[2] In addition, we take $k_{-1}/(k_4[CO])$ to be negligible and we assume k_{et} to be large (2×10^5 M^{-1} s^{-1} or larger gives the same results).[1]

The heterogeneous rate constants, k_h, are expressed in terms of the diffusion coefficient, D, as $k_h/\sqrt{D}$. As previously described,[1] for the couples $1/1^+$ and $2/2^+$, we obtained $k_h/\sqrt{D}$ (an effective value including solution resistance) and the transfer coefficient, α, using cyclic voltammetry (CV) and square wave voltammetry (SW). The values of $k_h/\sqrt{D}$ lie within the range 0.7–2 s$^{-1/2}$ cm^{-1}. The values of α lie between 0.4 and 0.5. In addition, we obtained the decomposition rate constants for the oxidized species, 1^+ and 2^+. For these two species (for a given ligand) the electrochemical parameters prove to be nearly identical. For example, parameters describing the electrode kinetics of the $1/1^+$ and $2/2^+$ couples (L = PPh$_3$) are $k_h\sqrt{D} = 0.85$ s$^{-1/2}$ cm^{-1}, $\alpha = 0.45$, $E^{\circ\prime} = 0.240$ V, with respect to a platinum pseudoreference electrode, and $k_h/\sqrt{D} = 1.0$ s$^{-1/2}$ cm^{-1}, $\alpha = 0.45$, $E^{\circ\prime} = 0.325$ V, respectively. A common value of D was employed for the all the species. Because [CO] was always more than 10 times larger than [η-Cp(CO)(L)FeMe], the error introduced is negligible. The simulations were done via the Adams–Moulton method with extrapolation to zero net size.[2]

We find that satisfactory simulation of the data over a wide range of [AN] is possible. Figure 2 shows a plot of the experimental and calculated current ratios, i_2/i_1, for a scan rate of 0.020 V s^{-1} as a function of [AN] for the complexes containing isosteric ligands P(*p*-XPh)$_3$. The results are shown in Table I. Uncertainties are discussed in refs 1 and 2. Estimated errors for k_3 and k_4/k_{-3} are less than 15%. In order to illustrate the sensitivity of the fit to the parameters, in Figure 2B, we show the effect of selecting two values (4 and 9 s^{-1}) for k_3 which differ from that (5 s^{-1}) reported in Table I. The ratio, k_4/k_{-3}, was adjusted to give the best fit of the calculated to experimental curves at low [AN]. Note that curves a and c depart from the experimental values at high [AN].

(4) (a) Liu, H.-Y.; Eriks, E.; Prock, A.; Giering, W. P. *Acta Crystallogr.* **1990**, *C46*, 51–54. (b) Panek, J.; Prock, A.; Eriks, K.; Giering, W. P. *Organometallics* **1990**, *9*, 2175. (c) Liu, H.-Y.; Eriks, E.; Prock, A.; Giering, W. P. *Organometallics* **1990**, *9*, 1758. (d) Eriks, K.; Liu, H.-Y.; Koh, L.; Prock, A.; Giering, W. P. *Acta Crystallogr.* **1989**, *C45*, 1683–1686. (e) Rahman, Md. M.; Liu, H.-Y.; Eriks, K.; Prock, A.; Giering, W. P. *Organometallics* **1989**, *8*, 1–7. (f) Rahman, Md. M.; Liu, H.-Y.; Prock, A.; Giering, W. P. *Organometallics* **1987**, *6*, 650–658. (g) Golovin, M. N.; Rahman, Md. M.; Belmonte, J. E.; Giering, W. P. *Organometallics* **1985**, *4*, 1981–1991. (h) Lezhan, C.; Poë, A. J. *Inorg. Chem.* **1989**, *28*, 3641. (i) Brodie, N. M.; Chen, L.; Poë, A. *Int. J. Chem. Kinet.* **1988**, *27*, 188. (j) Poë, A. J. *Pure Appl. Chem.* **1988**, *60*, 1209. (k) Dahlinger, K.; Falcone, F.; Poë, A. J. *Inorg. Chem.* **1986**, *25*, 2654. (l) Eriks, E.; Liu, H.-Y.; Prock, A.; Giering, W. P. *Inorg. Chem.* **1989**, *28*, 1759–1763.

(5) Bartik, T.; Himmler, T.; Schulte, H.-G.; Seevogel, K. *J. Organomet. Chem.* **1984**, *272*, 29.

(6) Tolman, C. A. *Chem. Rev.* **1977**, *77*, 313.

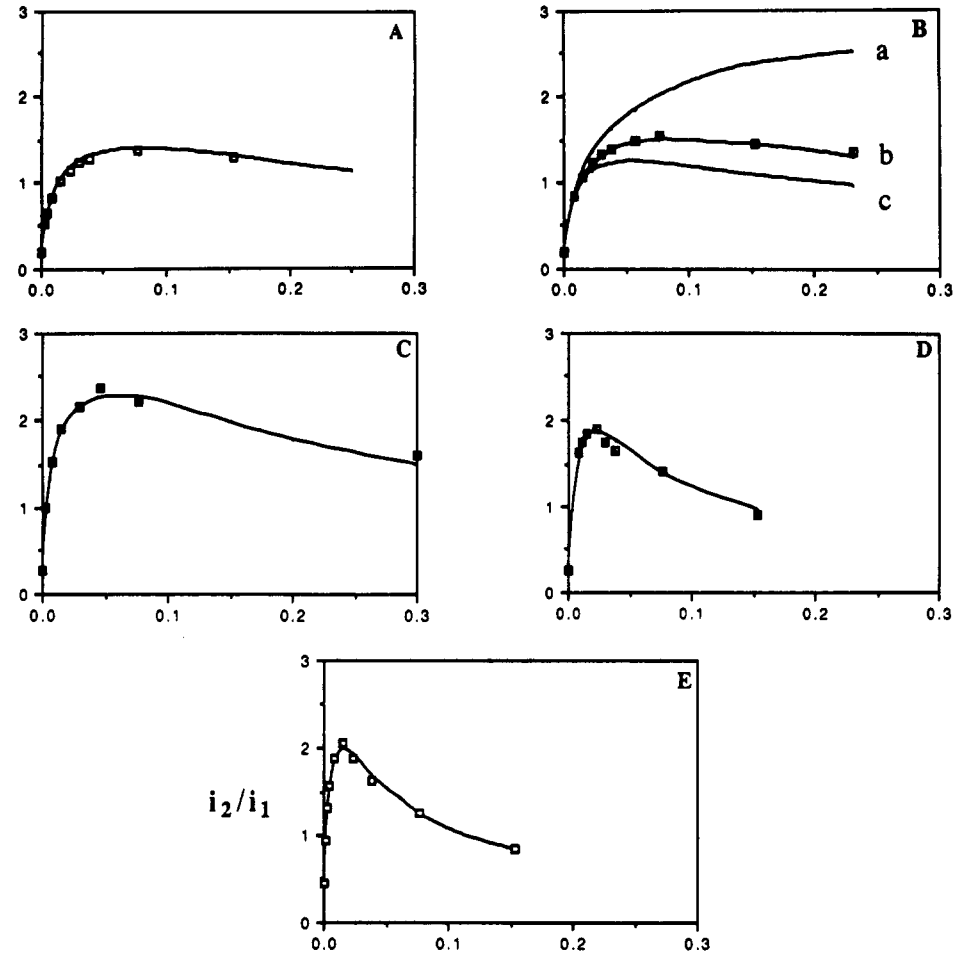

Figure 2. Plots of the experimental (squares) and calculated (solid line) SW current ratios versus [AN] in mL^{-1} for the anodic waves resulting from the oxidation of η-Cp(CO)(P(*p*-XPh)$_3$)FeMe (X = MeO (A), Me (B), H (C), F (D), Cl (E)) in mixtures of methylene chloride and acetonitrile (AN) containing 0.1 M TBAH under 1 atm of CO at 0 °C. The scan rate was 0.02 V s^{-1}. i_1 (see Figure 1) refers to the current resulting from the oxidation of η-Cp(CO)(P(*p*-XPh)$_3$)FeMe to η-Cp(CO)(P(*p*-XPh)$_3$)-FeMe$^+$, and i_2 refers to the oxidation of η-Cp(CO)(P(*p*-XPh)$_3$)FeCOMe (formed during the electrochemical experiment; see text) to η-Cp(CO)(P(*p*-XPh)$_3$)FeMe$^+$. In (B), curves a and c are based on values of 4 and 9 s^{-1} for k_3, respectively, and values of 20 and 0.7 for k_4/k_{-3}, respectively (see text).

Table I. Values of the Rate Constants and Ratios of Rate Constants for the Carbonylation of η-Cp(CO)(L)FeMe$^+$ As Shown in Scheme I with Data Measured on CH_2Cl_2 Solutions Containing 0.1 M TBAH at 0 °C under 1 atm of CO

L	χ^a	β^b	k_1[c,d]	k_2[e,f]	k_{-2}[c,f]	k_3[c]	k_4/k_{-3}	k_5[f]
PMe_2Ph	10.6	122	0.071	1.6×10^2	1.8	2.5	0.4	0.3
$PMePh_2$	12.1	136	0.059	1.7×10^2	1.3	2.0	0.4	0.35
$PEtPh_2$	11.3	140	0.039	68	1.3	6.0	0.5	1.2
P(*p*-MeOPh)$_3$	10.5	145	0.042	61	1.6	6.0	1.67	3.7
P(*p*-MePh)$_3$	11.5	145	0.047	77	1.6	5.0	2.0	2.8
PPh_3	13.25	145	0.067	1.9×10^2	1.4	6.0	2.0	1.8
P(*p*-FPh)$_3$	15.0	145	0.079	3.8×10^2	0.9	4.0	0.83	1.3
P(*p*-ClPh)$_3$	16.8	145	0.18	4.9×10^2	0.69	5.0	0.5	1.1
$PCyPh_2$	9.3	153	0.020	19	3.4	15	0.75	4.0
PCy_2Ph	5.35	161	0.027	2.7	6.0	35	1.0	5.1
PCy_3	1.4	170	0.024	0.55	7.1			18

[a] Data taken or calculated from data presented in ref 5. [b] Data calculated or taken from the data presented in ref 6. [c] First-order rate constants (s^{-1}). [d] Data taken from ref 1. [e] Second-order rate constants (M^{-1} s^{-1}). [f] Data taken from ref 2.

Results

The rates of carbonylation of the cation radicals, η-Cp(CO)(L)FeMe$^+$ (L = PMe_2Ph, $PMePh_2$, $PEtPh_2$, P(*p*-XPh)$_3$ (X = Me, MeO, H, F, Cl), $PCyPh_2$, PCy_2Ph, PCy_3), in CH_2Cl_2 (0.1 M TBAH, 0 °C, 1 atm CO) containing varying amounts of the coordinating solvent, AN, have been studied. For each of these complexes we find an increase in the rate of carbonylation which reaches a maximum at some [AN]. As an example, let us consider the redox-promoted carbonylation of η-Cp(CO)-(PPh_3)FeMe. The addition of small amounts of AN to a CH_2Cl_2 solution of η-Cp(CO)(PPh_3)FeMe causes a rather dramatic acceleration of the rate of carbonylation, which reaches a maximum (k_{obs} = 4.35 s^{-1}) at [AN] = 0.046 M (Figure 3). This corresponds to an enhancement of the rate of carbonylation by a factor of 65 relative to the rate of carbonylation in undiluted CH_2Cl_2. The rate of

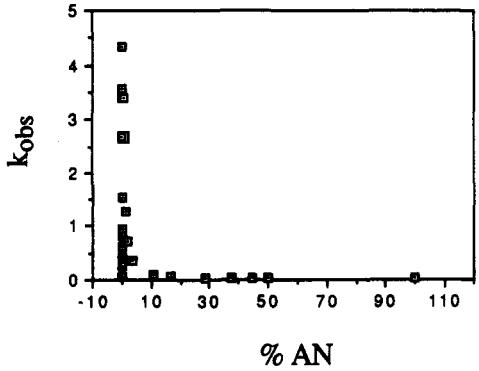

Figure 3. Plot of k_{obs} versus volume % of AN in CH_2Cl_2 for the conversion of η-Cp(CO)(PPh_3)$FeMe^+$ to η-Cp(CO)(PPh_3)-$FeCOMe^+$. See also Figure 2c, which shows an expanded region around the maximum i_2/i_1.

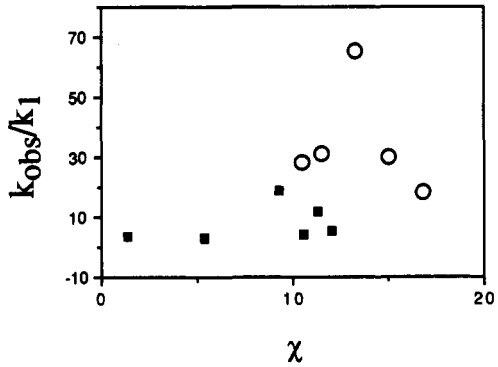

Figure 4. Plot of the maximum enhancement ratio (k_{obs}/k_1) for the conversion of η-Cp(CO)(L)$FeMe^+$ to η-Cp(CO)(L)-$FeCOMe^+$ versus χ. The data for the complexes containing P(*p*-XPh_3) are shown as open circles. The data for the remainder of complexes are displayed as solid squares.

carbonylation then declines and rapidly takes on the value observed when undiluted AN is the solvent.[7]

The other complexes behave in a similar manner except both magnitude of the enhancement (Figure 4) and the concentration of AN at which the maximum rate is observed (Figure 5) depend on the stereoelectronic properties of L. In particular, if we focus on the complexes containing the isosteric ligands, P(*p*-$XPh)_3$, we see that enhancement reaches a maximum for PPh_3 (Figure 4). In Figure 5 we have plotted [AN] where the maximum enhancement is observed versus the electronic parameter χ. It can be seen that the maximum enhancement occurs at progressively smaller [AN] as the electron donor ability of the L decreases (larger χ). (This can be seen in Figure 2, which show the plots i_2/i_1 (related to k_{obs}) versus [AN] for these complexes.) In fact, in a related study, we found

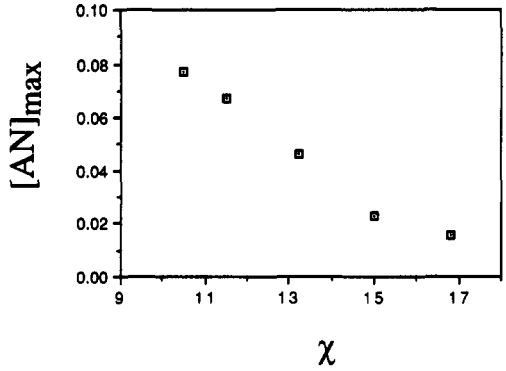

Figure 5. Plot of the [AN] where the enhancement of the rate of carbonylation of η-Cp(CO)(P(*p*-XPh_3))$FeMe^+$ is observed versus the electronic parameter χ.

that the enhancement effect vanishes for complexes containing the highly electrophilic trialkyl phosphites.[8] The shapes of the curves describing the relationship between i_2/i_1 and [AN] (for example, see Figure 2) change as the electron donor capacity of L changes. For the complexes containing the poorer electron donor L, the enhancement curves show a sharp spike after which the enhancement rapidly disappears. For the better electron donor ligands, the curves become progressively broader with a diffuse maximum that moves to higher concentrations of acetonitrile as the electron donor ability of L increases. This phenomenon has prevented us from obtaining satisfactory simulations of the electrochemical data for the PCy_3 complex, which is the best electron donor among the set of ligands.

We believe that the results of our electrochemical experiments are accommodated by the mechanism shown in the Scheme I. This scheme is based on the studies of the carbonylation of η-Cp(CO)(L)$FeMe^+$ in CH_2Cl_2 and in undiluted AN.

Discussion

Origin of the Enhancement of the Rate of Carbonylation. We initiated this research to answer the question as to the involvement of an intermediate in the transformation of 1^+ to 2^+ when carried out in undiluted AN.[2] The enhancement of the rate of carbonylation when small amounts of AN are added to methylene chloride reaction mixtures supports the existence of an intermediate, 4^+, and the opening up of the new pathway 1^+–3^+–4^+–2^+. In our model (Scheme I), the decrease in the carbonylation rate at higher concentrations of AN arises from the increasingly important reaction of 4^+ back to the AN complex, 3^+.

We can see how a maximum develops in the rate of enhancement as a function of [AN] if we consider the result of doing the reaction (Scheme I) for simplicity under homogeneous conditions using a chemical oxidant (e.g. 5% of the starting iron complex) to initiate the process. For example in the case of L = PPh_3, in a wide concentration region around the maximum rate, we may neglect the small contributions of the k_1 and k_5 steps (important only for CH_2Cl_2 or AN solution, respectively), and write

Scheme II

$$1^+ \underset{k_{-2}}{\overset{k_2[AN]}{\rightleftarrows}} 3^+ \underset{k_{-3}[AN]}{\overset{k_3}{\rightleftarrows}} 4^+ \xrightarrow{k_4[CO]} 2^+ \xrightarrow{k_{el}[I]} 1^+ + 2 \qquad (2)$$

(7) The acceleration of the alkyl to acyl rearrangement by nucleophilic solvents and solutes is well documented: (a) Cotton, J. D.; Markwell, R. D. *J. Organomet. Chem.* **1990**, *388*, 123 and references therein. (b) Therien, M. J.; Trogler, W. C. *J. Am. Chem. Soc.* **1987**, *109*, 5127. (c) Webb, S. L.; Giandomenico, C. M.; Halpern, J. *J. Am. Chem. Soc.* **1986**, *108*, 345–347. (d) Wax, M. J.; Bergman, R. G. *J. Am. Chem. Soc.* **1981**, *103*, 7028. (e) Martin, B. D.; Warner, K. E.; Norton, J. R. *J. Am. Chem. Soc.* **1986**, *108*, 33–39. (f) Nicholas, K. M.; Rosenblum, M. *J. Am. Chem. Soc.* **1973**, *95*, 4449–4450. (g) Bock, R. L.; Boschetto, J. R.; Rasmussen, J. P.; Demers, J. P.; Whitesides, G. M. *J. Am. Chem. Soc.* **1980**, *102*, 6887. (h) Cotton, J. D.; Kroes, M. M.; Markwell, R. D.; Miles, E. A. *J. Organomet. Chem.* **1990**, *388*, 133. (i) Cotton, J. D.; Markwell, R. D. *Organometallics* **1985**, *4*, 937. (j) Warner, K. E.; Norton, J. R. *Organometallics* **1985**, *4*, 2150. (k) Jablonski, C. R.; Wang, Y. P. *Inorg. Chim. Acta* **1983**, *69*, 147. (l) Cotton, J. D.; Crisp, G. T.; Latif, L. *Inorg. Chim. Acta* **1981**, *47*, 171. (m) Cotton, J. D.; Crisp, G. T.; Daly, V. A. *Inorg. Chim. Acta* **1981**, *47*, 165. (n) Mawby, R. J.; Basolo, F.; Pearson, R. G. *J. Am. Chem. Soc.* **1964**, *86*, 3994. (o) Caderazzo, F.; Cotton, F. A. *Inorg. Chem.* **1962**, *1*, 30.

(8) Unpublished results.

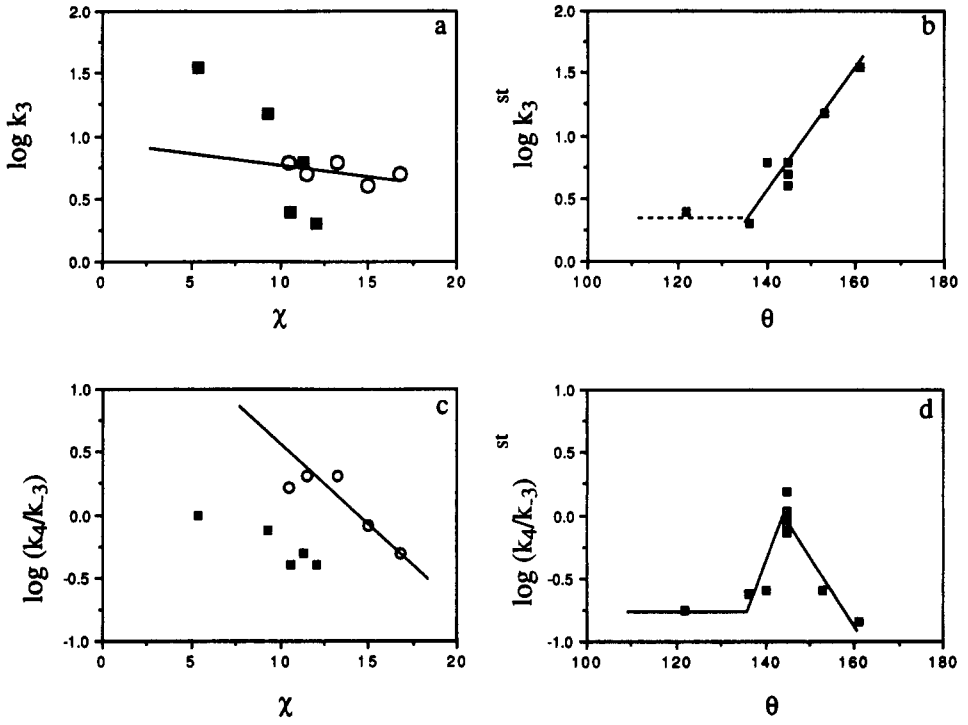

Figure 6. Electronic (a, c) and steric (b, d) profiles for the conversion of 3^+ to 4^+ (k_3 step in Scheme I) and the ratio k_4/k_{-3} for the partitioning of 4^+ between 2^+ and 3^+. The lines in the electronic profiles are drawn through the data for the complexes containing the isosteric ligands, P(*p*-XPh)$_3$. The intersections of the dashed and solid lines in the steric profiles indicates possible steric thresholds near 136° (b, d).

Because k_{et} is large and η-Cp(CO)(L)FeMe$^+$ is quickly generated from η-Cp(CO)(L)FeCOMe$^+$, a steady state is rapidly reached in [1^+], [3^+], and [4^+]. (This is borne out by direct computation.) Let C be the concentration of the added initial oxidant. Then

$$C = [1^+] + [3^+] + [4^+] \approx [1^+] + [3^+] \quad (3)$$

$$d[1^+]/dt = 0 = -k_2[AN][1^+] + k_{-2}[3^+] + k_4[CO][4^+] \quad (4)$$

$$d[4^+]/dt = 0 = k_3[3^+] - k_{-3}[AN][4^+] - k_4[CO][4^+] \quad (5)$$

$$\text{rate} = d[2]/dt = k_4[CO][4^+] = k_{obs}[CO]C \quad (6)$$

On solving for [4^+] and substituting into eq 6 we find

$$k_{obs}[CO] = \frac{\frac{k_2k_3}{k_3 + k_{-2}}[AN]}{\left(\frac{k_2}{k_3 + k_{-2}}[AN] + 1\right)\left(\frac{k_{-3}}{k_4[CO]}[AN] + 1\right)} \quad (7)$$

[AN] appears in the numerator and both factors of the denominator of eq 7. Thus, for very large or very small [AN], k_{obs}[CO] goes to zero. For an intermediate concentration of AN, k_{obs}[CO] passes through a maximum. The larger the ratios $k_2/(k_3 + k_{-2})$ and k_{-3}/k_4[CO], the smaller is [AN] at this maximum of k_{obs}[CO].

Does 3^+ Go Directly to 2^+ in Undiluted Acetonitrile? In a previous paper[2] we noted that a second-order reaction between 3^+ and CO could involve a direct reaction or could involve a rapid preequilibrium between 3^+ and an intermediate (4^+) which subsequently formed 2^+ as shown in Scheme I. Undoubtedly, the stepwise conversion of 3^+ and 2^+ is operative at low concentrations of AN. In undiluted AN, if the direct route were important, the rate of conversion of 3^+ to 2^+ (k_5) would be larger than that predicted for the stepwise process, $k_3k_4/(k_{-3}$[AN]). Indeed, we find that k_5 is up to eight times larger than $k_3k_4/(k_{-3}$[AN]). Although this might indicate that the direct route is more important in undiluted AN, this interpretation must be viewed with caution because the relatively large values of k_5 might be a consequence of the dramatic change in the solvent medium.

The situation is further complicated by the analysis of the ligand effect data (vide infra), which suggests that k_5 is a composite of k_3 and k_4/k_{-3}. This observation supports the notion that the path 1^+–3^+–4^+–2^+ is important even in undiluted acetonitrile. We hope that ongoing research will resolve this issue shortly.

Comments on the Possible Nature of Intermediate 4^+ and the Electronic and Steric Profiles of k_5 and k_4/k_{-3}. There are several reasonable candidates for 4^+ including η-Cp(CH$_2$Cl$_2$)(L)FeCOMe$^+$, η-Cp(PF$_6$)(L)-FeCOMe, and η-Cp(L)Fe-η^2-(COMe)$^+$. Analysis of the electronic and steric profiles[4] of k_3, k_4/k_{-3}, and k_5 sheds some light on the problem.

The electronic profile of the k_3 step (Figure 6) shows that the process is insensitive to the electron donor ability of L. This observation leads us to conclude that the electron density on the iron in the k_3 transition state is similar to that in 3^+. The steric profile shows that the k_3 reaction is sterically accelerated with a possible steric threshold near 135°. The lack of a second threshold in the k_3 step suggests that the transition state is less crowded and/or less rigid than η-Cp(AN)(L)FeCOMe$^+$. It appears that AN is extensively dissociated in the transition state of the k_3 step.

We believe that we can exclude η-Cp(CH$_2$Cl$_2$)(L)-FeCOMe$^+$ as 4^+ on the basis of the electronic and steric

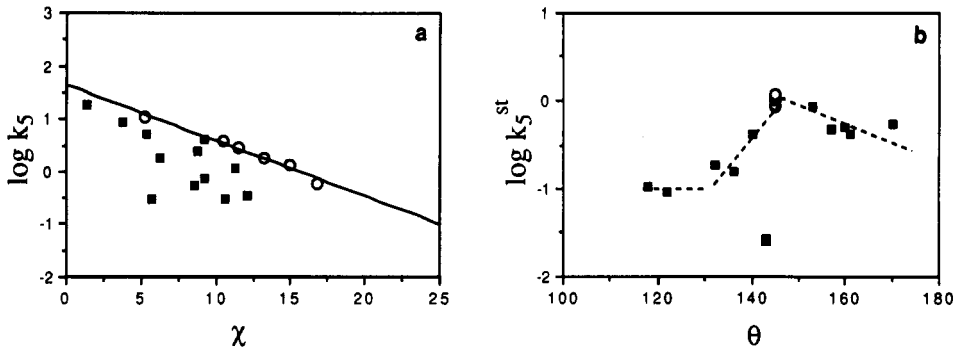

Figure 7. Electronic (a) and steric (b) profiles of k_5 step. The best fit line is drawn through the data for the complexes containing the isosteric ligands P(*p*-XPh)$_3$ (open circles).

profiles of the k_3 step. If the AN ligand of 3^+ were being displaced by CH_2Cl_2, then the loss of electron density at the iron caused by the departing AN would have to be compensated by the entering CH_2Cl_2. Intuitively we know that CH_2Cl_2 is a much poorer electron donor than AN, therefore Fe–CH_2Cl_2 bond formation would have to be more advanced than Fe–AN bond cleavage. Such a transition state would probably be crowded, and the reaction would show steric inhibition. Since the k_3 step shows steric acceleration, we exclude η-Cp(CH_2Cl_2)(L)-FeCOMe$^+$ as a choice for 4^+.

Analysis of the electronic and steric profiles of k_4/k_{-3} provides evidence against the intermediacy of η-Cp(L)-Fe-η^2-(COMe)$^+$. The electronic profile shows that the ratio is increased as the electron donor capacity of L increases. This seems reasonable since k_4, which involves the incorporation of CO into the complex, should be enhanced as the electron donor capacity of L increases. Likewise, the reversion of 4^+ and 3^+ by reacting with the electron-rich AN should be impeded (smaller k_{-3}, thus larger k_4/k_{-3}) by increasing electron donor capacity of L. So the electronic profile is consistent with identifying 4^+ as η-Cp-(L)Fe-η^2-(COMe)$^+$. The steric profile, however is inconsistent. The steric profile shows a rather sharp steric acceleration between 136 and 145° followed by an equally sharp steric inhibition. Although it is not clear as to how the k_4 and k_{-3} steps contribute to the steric profile, it does seem likely that the sharp inhibition of the reaction after θ = 146° is due to steric inhibition of the presumably associative reaction between 4^+ and CO. However, we expect η-Cp(L)Fe-η^2-(COMe)$^+$ not to be crowded and therefore not to show the sharp steric inhibition that is observed.

This leaves η-Cp(PF_6)(L)FeCOMe as a viable option. The displacement of the neutral AN by the anion, PF_6^-, might account for the electronic insensitivity of the k_3 step even if the Fe–AN bond cleavage is more advanced than the Fe–PF_6^- bond formation in the transition state. Second, it seems reasonable that the reaction of CO with a neutral complex (η-Cp(PF_6)(L)FeCOMe) would be more favored than reaction of CO with a cationic species. Third, the reaction of CO with η-Cp(PF_6)(L)FeCOMe might lead to a transition state with considerable Fe–CO bond formation and relatively little Fe–PF_6 bond cleavage. Such a transition state, which would maintain the neutral character of the complex, might be crowded and lead to the sharp steric inhibition after θ = 145°. A definitive answer to the question of the identity of 4^+ awaits the results of studies of the affect of supporting electrolyte on the kinetics of the carbonylation of η-Cp(CO)(L)FeMe.

Comparison of the Electronic and Steric Profiles of k_3, k_4/k_{-3}, and k_5. The electronic and steric profiles of the k_5 step (carbonylation of η-Cp(CO)(L)FeMe$^+$ in undiluted AN) (Figure 7) almost appears to be a composite of the electronic and steric profiles of k_3 and k_4/k_{-3}. For example the slope of the electronic profile for the k_5 step for the complexes containing the isosteric ligands P(*p*-XPh)$_3$ is nearly equal to the sum of the slopes of the analogous electronic profiles for k_3 and k_4/k_{-3}. Second, the steric profile of k_5 appears to be the composite of the k_3 and k_4/k_{-3} steric profiles. Thus, analysis of the electronic and steric profiles provides evidence that the stepwise carbonylation pathway, 1^+–3^+–4^+–2^+, is operative even in undiluted AN.

Conclusion

The carbonylation of η-Cp(CO)(L)FeMe$^+$ in mixtures of methylene chloride and acetonitrile is noteworthy since it is the only system of which we are aware where the individual steps in the carbonylation process (Scheme I) can be probed systematically. It is also noteworthy, although not surprising, that the individual steps exhibit different stereoelectronic demands on phosphorus(III) ligands. For example, the k_2 step is dominated by electronic factors, whereas the k_3 step is dominated by steric factors. In principle, it is possible to express quantitatively the various rate constants in terms of stereoelectronic properties of L. It would be possible then to predict quantitatively the combination of stereoelectronic properties of L that would lead to the maximum rate of carbonylation. Research directed toward this type of rational choice of ligands is in progress.

Ongoing research has shown that the acceleration of the reaction by acetonitrile pales in comparison to that which can be obtained using other nucleophilic solvents such as acetone or THF. Studies of rate enhancements by these solvents will be reported in the future.

Acknowledgment. We gratefully acknowledge the donors of the Petroleum Research Fund, administered by the American Chemical Society, for support of this work.

Supplementary Material Available: A listing of the computer code used for the simulation of the electrochemical experiments described in this paper (7 pages). Ordering information is given on any current masthead page.

OM920415W